Two-Dimensional Mapping of Photon Counts in Low-Noise Single-Photon Avalanche Diodes

Jau-Yang Wu*, Shu-Cheng Li, Fang-Ze Hsu, and Sheng-Di Lin

Department of Electronics Engineering, National Chiao Tung University, Hsinchu 300, Taiwan

**Corresponding Author: judewu13.ee97g@nctu.edu.tw , telephone: +886-3-5712121ext54240*

***Abstract*---We characterize the 2-D spatial distribution of photon counts inside the active area of low dark-count-rate single-photon avalanche diodes. The 2-D mappings are measured with various wavelengths and excess voltages. A non-uniform distribution of photon detection probability is spotted at high voltages. Our results reveal that the engineering of electric field is of importance for high performance SPADs.**

I. Introduction

Recently, planar CMOS single photon avalanche diodes (SPADs) emerge as potential devices for high-speed detection of ultra-weak light by taking place of photon multiplier tubes and charge-coupled devices [1]. Thanks to the standard planar CMOS technology, silicon SPADs were taped out as imager with time to digital (TDC) circuits on chip, which can be applied to the study of time-correlated single photon counting in fluorescence lifetime image microscopy [2] and 3-D imaging [3]. In addition, customized SPADs with high photon detection efficiency bonded with CMOS timing circuits forms a focal plane array chip [4], or adapted with outside TCSPC module [5] were applied in long range finding applications, such as Laser Detection And Ranging (LADAR).

In a SPAD under the Geiger mode operation, a photo-generated carrier accelerated by high electric field can trigger an avalanche event, which makes avalanche diodes arriving at single photon counting. The photon detection process includes light absorption, carrier transport, and avalanche multiplications. The process depends on not only the device structure but also the electric field which is position-dependent. Therefore, understandings of the spatial distribution of electric field are essential for designing high detection efficiency SPADs. In this work, we setup a measurement system to map the 2-D spatial distribution of photon counts of a SPAD, and simulate the distributions of electric field with the software of technology computer-aided design (TCAD). The experimental data reveal a non-uniform distribution of photon detection efficiency. Comparing the observation with the simulation results, it shows that connecting metal layer above the active region causes the non-uniformity of electric field distribution so the photon count is position-dependent.

II. Device description

The SPAD is fabricated in TSMC 0.25-μm standard high-voltage CMOS technology and the device structure is schematically illustrated in Fig. 1(a). The guard-ring free active region is formed by the junction between the high-voltage p-well (HVPW) and the n-typed buried layer (NBL). The device with circular shape of 20-μm diameter (the inset of Fig. 1(b)) has a breakdown voltage (V_b) of around 75.4 V as shown in the I-V curve in Fig. 1(b).

To measure the dark count rate (DCR), a passive quenching circuit consisting of a 200 kΩ resistor in series is used to quench the avalanche current. The avalanche current pulses are sensed through an ac coupled capacitor (10 nF), amplified by a signal amplifier and then counted by a counter. As shown in Fig. 2, the devices exhibit a very low dark count rate of less than 1 kHz even at an excess bias (V_e) of 7.0 V, which has been discussed previously [6].

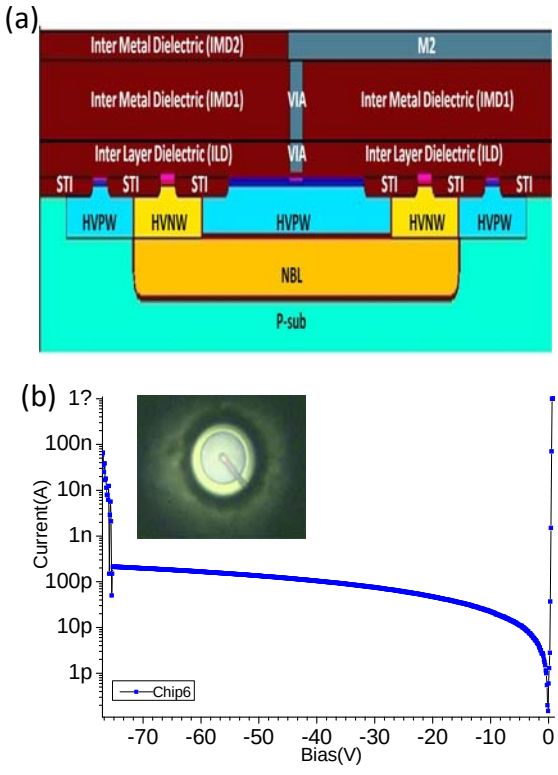

Fig. 1 (a) Cross-section of our SPAD ;(b) I-V curve of the SPAD. The inset shows its top-view picture taken by optical microscope.

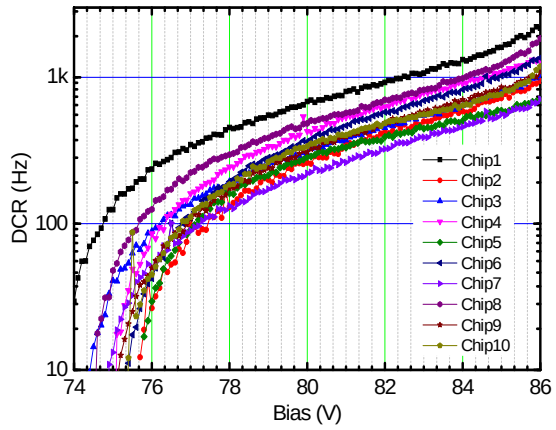

Fig. 2 Measured dark count rates of ten devices as a function of bias voltages.

III. Measurement system

To characterize the photon detection efficiency (PDE) of SPADs, a 1000W halogen light source (ORIEL-66188) was first dispersed by a monochromator (HR-550) and transmitted into a microscope through a large core fiber in a dark box. The incident photon flux is real-time monitored by a calibrated photodiode (Thorlabs FDS100-CAL). With a zero aperture iris on the microscope and 100X NIR objective lens, we can shrink the spot size to be smaller than 1 μm. To perform high-precision 2-D mapping of photon counts in the active area of devices, a high-precision stage (Newport 562) driven by two individual high resolution actuators (Thorlabs Z825B) are set up and controlled by a computer, as show in Fig 3.

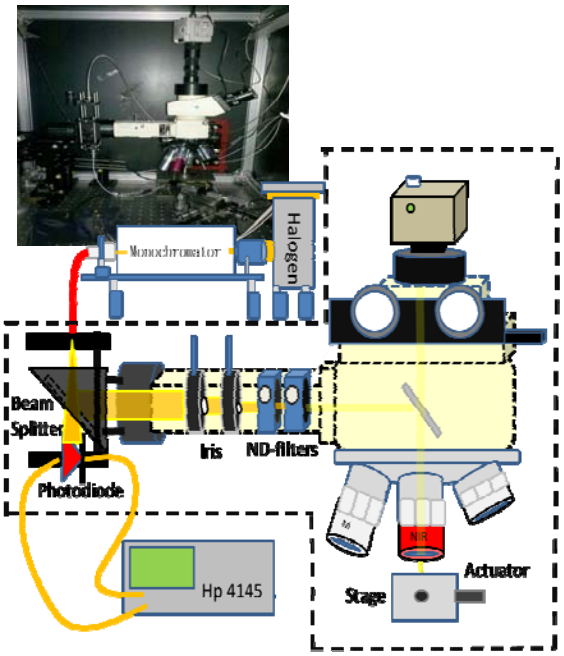

Fig. 3 Schematic measurement system in dark box and its photo picture (left-top).

When proceeding PDE and 2-D mappings of photon counts measurement, we make the shutter in the front of monochromator on and off in turns so the light and dark counts can be measured under the same condition. Since the light spot was too small to define the photon flux, we present the photon counts to instead of PDE in 2-D mapping measurement. On the other hand, in the PDE measurement, the spot size is set to the same as the diameter of active region for preventing the carriers diffusion coming from other regions.

IV. Results and discussions

As indicated in Fig. 4, at an excess bias of 10.1 V, the PDE of our SPAD has a peak of 12.3% at the wavelength of 510 nm. Clear oscillations of PDE are observed at all bias voltages, which are attributed to the interference of the dielectric layers above the device.

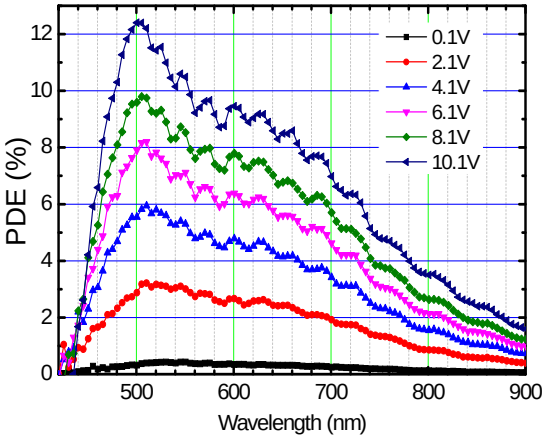

Fig. 4 Measured PDE as a function of wavelength under various excess bias voltages.

In Fig. 5, 3-D plot shows the measured photon count distribution in the active region. A clear ring-like non-uniform distribution is spotted for the incident light of 500-nm wavelength at the excess bias of 9.0 V. To study the non-uniformity, the 2-D mappings of normalized photon counts at various excess biases for the wavelengths of 500, 625, and 750 nm are measured and the results are plotted in Fig. 6. Note that the p^+ contact pad is connected from the center to the bottom-right, as shown in the inset of Fig. 1(b). Let us look at the first column for 500 nm. The photon counts exhibit a non-uniform distribution over the active area and become more serious as increasing the excess bias. Besides, under the same excess bias, the uniformity restores at longer wavelength (within the same row in Fig. 6). The region having lower photon counts is not only caused by the light shielding of the metal. Considering that different wavelength gives maximum absorption at different depth, the non-uniformity of photon counts distribution can be

attributed to the depth dependence of the electric field. We suspect that the non-uniform distribution results from the electric field distribution inside the device.

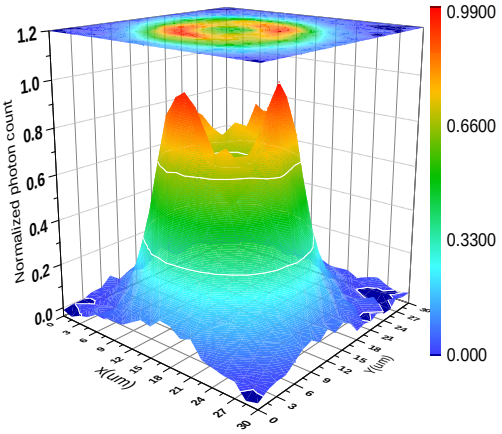

Fig. 5 3-D plot of 2-D mappings for incident light of 500 nm under excess biases of 9V

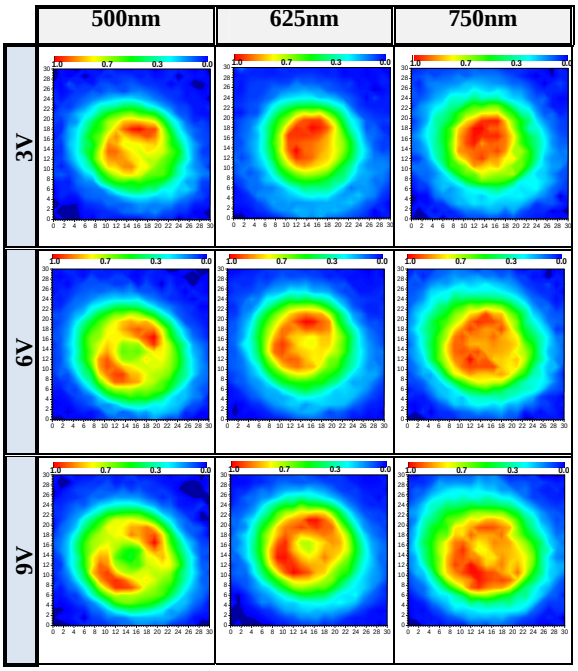

Fig. 6 2-D mappings of photon counts for 500, 625, and 700 nm under excess biases of 3, 6, and 9 V.

To explain the observation, we simulate the electric field distribution of the SPAD by using the commercial software, Synopsys Sentaurus TCAD, and the results are presented in Fig. 7. The high electric field is located near the HVPW/NBL junction, as expected (Fig. 7(a)). To make it clear, we plot the *x*-dependent electric field at various depths in Fig. 7(b). First, the electric field indeed peaks near the edge of the active region. Second, the peak electric field at the left side (no metal above) is a bit higher than that at the right side (underneath the metal). Third, the non-uniformity of the electric field becomes more serious with the shallower depths (more negative depths) as it comes near to the metal layer. High electric field gives higher trigger probability so the photon counts increase. This explains why the distribution of photon counts is more uniform for longer wavelength. This result indicated that, by mapping the photo counts distribution with various wavelengths, we can probe the 3-D electric field distribution in the device.

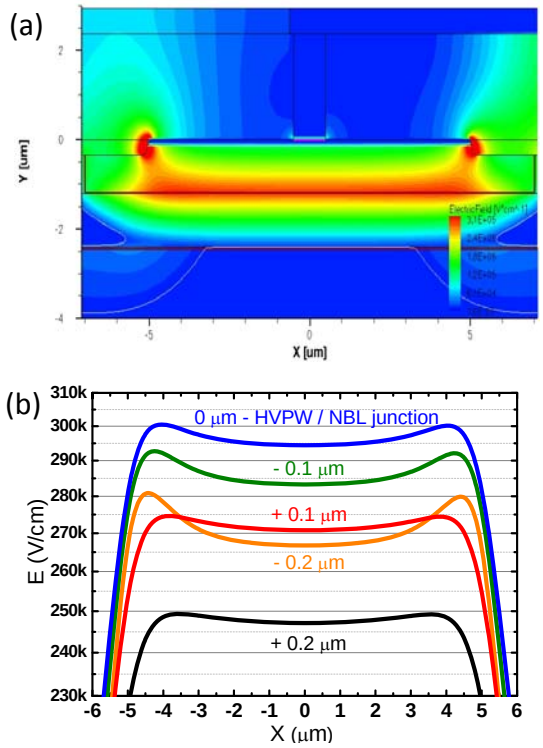

Fig. 7 Simulation of electric field distributions at excess bias of 9 V ;(a) 2-D contour and (b) *x*-dependence at various depths. Note that the more negative depth means closer to the device surface.

In Fig. 8, we plot the electric field non-uniformity in a quantitative way to reveal the effect of the bias voltage. The maximum electric field on the left side (E_L) subtracted with the minimum in the middle (E_M) divided by the minimum in the middle are plotted against the excess voltages in Fig. 8(a). Similar comparison between left and right side maximums are plotted in Fig. 8(b). Clearly, with the increasing bias voltages, the non-uniformity becomes more significant. Both Figs. 8(a) and 8(b) reveal that deeper depths restore the uniformity of electric field. It is because, for a more distant position, the metal layer has less effect on the electric field there, which is consist with our observation with long-wavelength light.

Acknowledgement

We are grateful to the National Center for High performance Computing for computer time and facilities and the National Chip Implementation Center (CIC) for help on chip fabrication. This work was financially supported by the NSC and ATU

program of MOE in Taiwan.

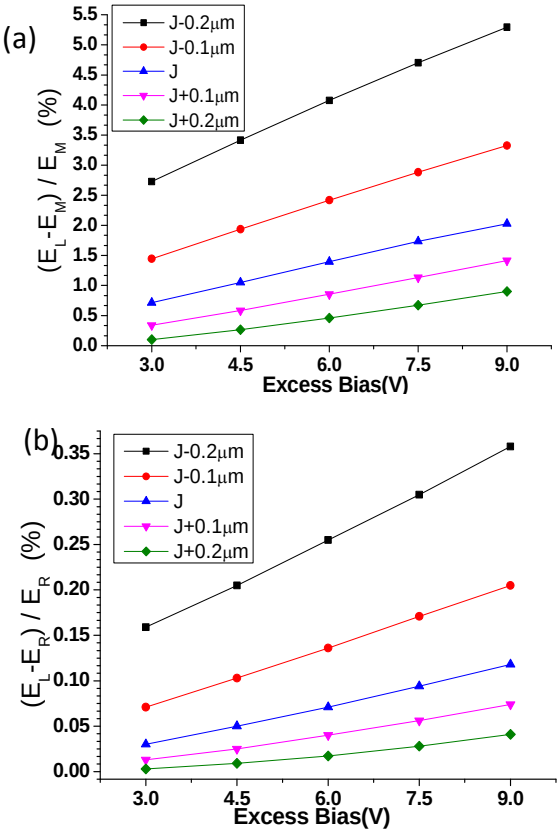

Fig. 8 Maximum electric field on the left side difference ratio with respect to (a) the minimum in the middle and (b) the maximum on the right side.

References

[1]. A. Rochas, A.R. Pauchard, Pierre-A Besse, D. Pantic, Z. Prijic, R.S. Popovic, "Low-noise silicon avalanche photodiodes fabricated in conventional CMOS technologies," IEEE Trans. Electron. Dev., vol. 49, no.3, pp.387-394, March 2002.

[2]. M. Gersbach, Y. Maruyama, R. Trimananda, M. W. Fishburn, D. Stoppa, J. A. Richardson, R. Walker, R. Henderson, E. Charbon, , "A Time-Resolved, Low-Noise Single-Photon Image Sensor Fabricated in Deep-Submicron CMOS Technology," IEEE J. Solid-State Circuits, vol. 47, no. 6, pp.1-14, June 2012.

[3]. C. Niclass, K. Ito, M. Soga, H. Matsubara, I. Aoyagi, S. Kato, and M. Kagami, "Design and characterization of a 256 × 64-pixel singlephoton imager in CMOS for a MEMS-based laser scanning time-of-flight sensor," Opt. Express, vol. 20, no. 11, pp. 11863–11881, May 2012.

[4]. R. Heinrichs, B. F. Aull, R. M. Marino, D. G. Fouche, A. K. McIntosh, J. J. Zayhowski, T. Stephens, M. E. O'Brien, M. A. Albota, "Three-dimensional laser radar with APD arrays." Proc. SPIE vol. 4377, pp. 106-117, 2001.

[5]. N. J. Krichel, A. McCarthy, A. M. Wallace, J. Ye, G. S. Buller, "Long-range depth imaging using time-correlated single-photon counting. " Proc. SPIE vol. 7780, 77801I 1-12, 2010.

[6]. F. Z. Hsu, J. Y. Wu, S. D. Lin, "Low-noise single-photon avalanche diodes in 0.25 μm high-voltage CMOS technology," Opt. Lett., vol. 38, no. 1, pp. 55-57, January 2013.